PID 29197

Flame Inhibition by Phosphorus-Containing Compounds in Lean and Rich Propane Flames

O.P. Korobeinichev, V. M. Shvartsberg, A.G. Shmakov, T.A. Bolshova

Institute of Chemical Kinetics & Combustion
Novosibirsk, 630090 Russia

T.M. Jayaweera, C. F. Melius, W.J. Pitz, C.K. Westbrook*

Lawrence Livermore National Laboratory
PO Box 808, Livermore, CA 94551-0808 USA

H. Curran

Department of Chemistry
National University of Ireland, Galway
Galway, Ireland.

Short Running Title: Flame Inhibition by Phosphorus Compounds

*corresponding author
Charles K. Westbrook
L-090
Lawrence Livermore National Laboratory
7000 East Avenue
P. O. Box 808
Livermore, CA 94550 USA
Tel: 925-422-4108
Fax: 925-422-2644
Email: westbrook1@llnl.gov

ABSTRACT

Chemical inhibition of laminar propane flames by organophosphorus compounds has been studied experimentally and computationally using a detailed chemical kinetic reaction mechanism. Both fuel-lean and fuel-rich propane flames were studied to examine the role of equivalence ratio in flame inhibition. The experiments examined a wide variety of organophosphorus compounds. We report on experimental species flame profiles for tri-methyl phosphate (TMP) and compare them with modeled species flame profile results of TMP and di-methyl methyl phosphonate (DMMP). Both experiments and kinetic modeling indicate that inhibition efficiency is effectively the same for all of the organophosphorus compounds examined, independent of the molecular structure of the initial inhibitor molecule. Chemical inhibition is due to reactions involving small P-bearing species $HOPO_2$ and HOPO produced by the organophosphorus compounds (OPCs). Ratios of $HOPO_2$ and HOPO concentrations differ between lean and rich flames, with $HOPO_2$ dominant in lean flames while HOPO dominates in rich flames. Resulting $HOPO_2$ and HOPO species profiles do not depend significantly on the initial source of the $HOPO_2$ and HOPO and thus are relatively insensitive to the initial OPC inhibitor. A more generalized form of the Twarowski mechanism is developed to account for the results observed, and new theoretical values are determined for heats of formation of the important P-containing species, using the BAC-G2 method.

Keywords: Phosphorus, inhibition, premixed flames, thermochemistry, modeling

Introduction

For many years, halogenated hydrocarbons, especially CF_3Br, were used as the preferred means of fire suppression, until their role in atmospheric ozone depletion limited their use with the 1990 Montreal Protocol. The search for effective replacements has led to a family of organophosphorus compounds (OPCs) which show considerable promise as flame inhibitors [1]. Early work of Twarowski [2-4] showed that phosphine (PH_3) accelerated radical recombination in hydrogen oxidation, and subsequent work by Korobeinichev et al. began to explain how other OPCs inhibited hydrogen [5,6] and hydrocarbon flames [7].

Chemically active flame inhibitors alter flame chemistry by catalytically recombining key flame radicals, especially H and O atoms and OH radicals. Fast elementary reactions interconnect these small radical species, and removal of any of them through recombination reduces concentrations of all of them correspondingly. Therefore, radical recombination leads to fewer H atoms in the reaction zone, which leads to reduced chain branching through the reaction $H+O_2 = O+OH$, and a lower burning velocity. This applies to familiar halogenated suppressants such as HBr and CF_3Br [8,9], sulfur compounds such as SO_2 [10,11], and OPCs such as dimethyl methylphosphonate (DMMP) and trimethyl phosphate (TMP).

Twarowski [2-4] established that catalytic recombination of radicals by phosphine (PH_3) is accomplished by reactions of small P-containing species produced from the additive, particularly

$$H + PO_2 + M \rightarrow HOPO + M \qquad (1a)$$

$$HOPO + H \rightarrow H_2 + PO_2 \qquad (1b)$$

$OH + PO_2 \ (+ M) \rightarrow HOPO_2 \ (+ M)$ (2a)

$H + HOPO_2 \rightarrow H_2O + PO_2$ (2b)

which consume highly reactive H atoms and OH radicals to produce stable H_2 and H_2O. In most kinetic modeling studies of inhibition by OPC additives, an additional reaction between HOPO and OH to produce PO_2 and water is also included. The same small species act [12-26] with other parent OPCs such as TMP, DMMP, and in chemical warfare agents such as sarin.

Most investigations of flame inhibition by OPCs have been carried out in static or flow reactors in which diffusional transport is not important, or in stoichiometric flames. The present study examines the effect of fuel/oxygen ratios on chemical kinetics of inhibition by OPCs in laminar flames and how that suppression changes for different equivalence ratios and different OPCs. In lean hydrocarbon flames, OH radicals and O atoms normally dominate the radical pool while H atoms are most prevalent in rich conditions. Thus, it is possible that different reaction cycles may be responsible for flame inhibition at different equivalence ratios.

We therefore investigated flame inhibition kinetic pathways for rich and lean propane flames, using TMP and DMMP as flame inhibitors. A key is identification of P-containing species (PO_xH_y) involved (e.g., reactions 1 and 2 above). Past kinetic studies of flame inhibition by OPCs have been limited by lack of reliable experimental data for PO_xH_y species concentrations. For example, Noguiera and Fisher [18] compared measured only hydrocarbon species profiles from a DMMP-doped CH_4/air premixed flame to numerical model predictions. Significant differences between experimental and numerical results were observed, but errors could not be reduced since P-containing species concentrations could not be measured.

The present work reports results from experimental studies of premixed laminar propane flames carried out in the laboratory of O. Korobeinichev. Spatial profiles of major species concentrations were measured, including important OPCs. Fuel-lean and fuel-rich equivalence ratios and a wide variety of OPC inhibitors were employed. We focus on experimental results for undoped propane flames and the same flames doped with TMP. An existing chemical kinetic model was updated, including new PO_xH_y thermochemistry, to describe the experimental results and provide insights into OPC-doped flame inhibition.

Experiments

Premixed laminar flames were stabilized on a flat Botha-Spalding flat-flame burner 16 mm in diameter at atmospheric pressure and slightly elevated unburned gas temperatures of about 380K. Combustible $C_3H_8/O_2/Ar$ mixtures (lean, 0.025/0.136/0.839, $\phi \sim 0.9$, and rich, 0.029/0.121/0.85, $\phi \sim 1.2$) were prepared using mass flow controllers, with a total volumetric flow rate of 1.5 L/min at STP. TMP (1200 ppm) was added to the combustible mixtures using a saturator with liquid TMP in a controlled temperature bath. Temperature profiles were measured by Pt-Pt+10%Rh thermocouples welded from wire 0.02 mm in diameter, covered by a thin layer of SiO_2 to prevent catalytic recombination of radicals on their surfaces. The resulting thermocouple junction has a diameter of 0.03 mm and a shoulder length of about 3 mm, providing negligible heat losses to the cold contacts. Further details of the thermocouple design can be found in [5].

Chemical species profiles were measured by MBMS, using soft ionization by electron impact [19]. Synchronous demodulation was applied to measure flame species in low

concentration up to 10 ppm with a mean square error not more than 50%, and stable species with standard deviations not more than 10%. Quartz cones with inner angles of 40° and 45°, wall thickness of 0.05 mm and orifice diameter 0.05 – 0.09 mm were used as probes. In these atmospheric pressure experiments, the lifetime of the quartz probe is limited by the formation of a solid film of pyrophosphoric acids, especially near the probe tip, which alloys with heated quartz to form easily melted phosphate glass. Disturbance of the flames by the probe has been taken into account [27].

In separate experiments, the laminar burning velocity of premixed C_3H_8/air flames was measured using a Mache-Hebra nozzle burner [28] and the total area method from an image of the flame [29]. The obtained result of 41.7 cm/s for a stoichiometric undoped flame agrees well with experimental data measured by different techniques [30-32] and the computed value described below.

Modeling Approach

The Chemkin Premix code [33] was used to compute species profiles and reaction fluxes for burner-stabilized and freely propagating laminar flames. Experimentally measured temperatures were used as input for the burner-stabilized flames. A recent propane oxidation mechanism [34] was used for the hydrocarbon species. At atmospheric temperature and pressure, this mechanism computes a laminar burning velocity of 41.1 cm/s, in good agreement with our own experimental values above and other experimental studies.

Improvements in thermochemistry for the phosphorus compounds used the BAC-G2 method [35]. Enthalpies of formation for small phosphorus species are summarized in Table 1,

including values using other quantum chemical methods, including BAC-MP4 by Melius [36], G3X by Mackie et al. [37] and CBS by Bauschlicher [38].

Our kinetic reaction mechanism is based on previous models [12,13,17,22,23] for combustion inhibition with OPCs. Hydrocarbon reactions in each model differ slightly, and the reactions by which the initial OPC consumption occurs also differ slightly, but all are based on the reaction cycles identified originally by Twarowski.

A major change we have made is to refine the reaction kinetic pathway by which $HOPO_2$ can be converted to PO_2 and H_2O, clarifying the meaning of reaction 2b above. Like other apparently simple reactions, the reaction of H with $HOPO_2$ actually proceeds by a complex process, adding the H atom to the $HOPO_2$ species, forming an adduct in a metastable, excited energy state. The reaction then proceeds on a potential energy surface with multiple local potential energy minima. Each minimum defines a distinct metastable arrangement of the adduct species. A metastable species can be collisionally stabilized, or it can continue to rearrange itself in a number of possible ways, and it can complete the overall reaction by breaking into final, relatively stable products. For the reaction of H with $HOPO_2$, the H atom can add directly to the phosphorus atom in $HOPO_2$ to form HPO(OH)O, followed by a 1,2-hydrogen shift to form $PO(OH)_2$, and then a four-centered water elimination step to produce H_2O and PO_2. The initial addition step has no activation energy barrier, while the hydrogen shift and water elimination have barrier heights of about 4 kJ/mol above the reactants' energy. The reaction sequence is

$$HOPO_2 + H \leftrightarrow HPO(OH)O \leftrightarrow PO(OH)_2 \rightarrow H_2O + PO_2 \quad (2b')$$

in which some of the steps are reversible because they represent further rearrangements on the potential energy surface. We calculated the highest energy barrier between reactants and products of reaction 2b' to be less than 8.4 kJ/mol. To our knowledge, 2b' has not previously been proposed as a viable reaction pathway for this reaction, and since it has little or no activation barrier, it was found to be an important contributor to flame inhibition kinetics.

A different initial reaction step, where the H atom adds directly to one of the O atoms in $HOPO_2$, results in $PO(OH)_2$, followed by the same four-center water elimination step to produce H_2O and PO_2. This sequence can be represented

$$HOPO_2 + H \leftrightarrow PO(OH)_2 \rightarrow H_2O + PO_2 \qquad (2b'')$$

The energy barrier to this reaction pathway has recently been computed by Mackie et al. [37] to be approximately 51 kJ/mol.

If reactions 2b' and 2b" were irreversible and went directly to their products $H_2O + PO_2$, then both could be written as single-step reactions. The highest energy barrier in each sequence of steps would be the overall activation energy, with an A-factor determined by comparison with experiments or chemical theory. Twarowski and other early modeling studies used an equivalent approach by assuming from the begininning that this was an elementary reaction. Twarowski assumed a rate expression of 2×10^{13} exp(-50 /RT) and found rates of radical consumption that agreed with observations. The 50 kJ/mol is remarkably close to the value derived theoretically by Mackie et al. Twarowski's value for this reaction rate was used until the present, with minor modifications, although Korobeinichev et al. [20] carried out preliminary computations with a considerably lower A-factor, and then later [22] restored it to a value close to its value in the present model.

The present study used a related approach in its implementation of the reaction of H with $HOPO_2$. We included reaction 2b' as a single step reaction producing $H_2O + PO_2$ but using an energy barrier of zero to reflect the energetics of the reaction path through the HPO(OH)O intermediate. We also included reaction 2b", but we implemented it in two steps, the first producing $PO(OH)_2$ and the second step continuing to $H_2O + PO_2$. We did this because it appears that the intermediate $PO(OH)_2$ can react with radical species on times scales comparable with its 4-center water elimination reaction. The rate of the first step of reaction 2b" is very similar to that originally proposed by Twarowski, but with an activation energy of 37.7 kJ/mol, from our BAC-G2 thermochemical calculations.

In a particularly elegant recent theoretical study, Mackie et al. [37] introduced the concept of reaction 2b proceeding through an intermediate activated complex and identified that complex as $PO(OH)_2$. Their goal was to identify possible reaction pathways for small P-containing species that were more rapid than the simplified overall reaction steps. Our rate expression for the Mackie et al. reaction path agrees well with their calculations. Our identification of another, even lower energy barrier pathway provides another fast route for the second half of the catalytic inhibition cycle 2 and contributes significantly to computed results in this study.

It now appears that none of the other 3 reactions identified by Twarowski, reactions 1a, 1b and 2a, are likely to proceed as elementary reactions and require further theoretical study. Recently, Haworth et al. [39] presented theoretical analyses of these reactions with predictions of reaction rates under flame conditions, which will be very helpful in future modeling analyses.

We also added reactions involving the diphosphorus oxide compounds P_2O_3, P_2O_4 and P_2O_5, which have relatively strong bond-dissociation energies of 322, 310 and 385 kJ/mol, respectively (see Table I), to asses their role in the overall chemical kinetics. The entire hydrocarbon and OPC reactions mechanism can be obtained electronically at http://www-cms.llnl.gov/combustion/combustion_home.html.

Results and Discussion

This kinetic model was used to calculate the structures of the lean and rich propane flames, with and without 1200 ppm TMP in the unburned gases. Computed results for major reactant and product species and the spatial extent of each flame were in excellent agreement with experimentally observed values, shown in Figs. 1 and 2.

Computed and experimental species mole fractions for P-bearing species in the lean and rich inhibited flames are shown in Figs. 3 and 4. Overall agreement between experimental and computed values is very good for all of the species in the lean flame. However, there are significant disparities between model results and experimental data in the rich flame. To ensure that all possible P-bearing species were included, we included the P_2O_3, P_2O_4 and P_2O_5 species within the model. We found that their concentrations were insignificant (several orders of magnitude smaller than the PO, PO_2 and PO_3 species), in the lean and rich flames and cannot account for discrepancies in the rich flame. Low concentrations of the diphosphorus species are due to high product temperatures and low partial pressures of the phosphorus oxides. At higher dopant concentrations and flame pressures, diphosphorus species could become important.

We found that the POxHy species reach thermochemical equilibrium values at large distances from the burner. Good agreement between theory and experiment in the lean flame (Fig. 3) appears to validate thermochemistry for the POxHy species predicted by the BAC-G2 method (Table I). However, agreement for the rich flame (Fig. 4) is not as good. At large distances from the burner, we expect the POxHy species ratios to be at their thermodynamic equilibrium, not depending on the reaction mechanism. Given good agreement for the lean flame, we believe the modeled ratios of the POxHy species to be more reasonable, since the model uses the same thermochemistry for both flames. However, modeling results for the POxHy species profiles in the region near the reaction zone are quite sensitive to slight modifications in the reaction mechanism. Further studies, of both experimental profile measurements and the computational reaction mechanism, must be carried out to determine the cause of the differences.

To further understand the nature of the P-bearing species with respect to the inhibition mechanism, we also considered other OPCs. A recent study [40] showed that many different organophosphate compounds are approximately equal in inhibition effectiveness for hydrocarbon flames, as illustrated in Fig. 5, showing relative reductions in burning velocity from addition of other inhibitors to a stoichiometric propane/air mixture. Burning velocity reductions produced by other OPC additives, many of them including F atoms in addition to P atoms (one of them is shown in Fig. 5) were very similar to the purely OPC results shown here. These results are compared to reductions in burning velocity produced by addition of CF_3Br, which is much less effective than any of the OPC additives, and inhibition produced by addition of iron pentacarbonyl, which is much more effective.

To investigate inhibition similarities of different OPCs, we modeled the same propane/O_2/Ar flames but used DMMP as the dopant rather than TMP. Resulting P-bearing species profiles in the DMMP-doped flames are compared with those from the TMP-doped flames in Figs. 6 and 7 for the lean and rich flames. Similarities in P-bearing species mole fractions in these flames are striking. In both lean and rich pairs of flames, both additives are consumed at exactly the same rates, and levels of PO_2, HOPO and $HOPO_2$ are also effectively equal in the two flames and eventually reach exactly the same equilibrium levels in the burned gases.

These similarities are perhaps unexpected, since TMP decomposes primarily to produce $HOPO_2$, while HOPO is the primary product of DMMP (see Figs. 5 and 6 of [12]). Yet in spite of differences in initial decomposition products of the OPCs, both inhibited lean flames show predominant formation of $HOPO_2$, while rich flames show mostly formation of HOPO. Slight differences in Figs. 6 and 7 between TMP- and DMMP- inhibited flames represent residual effects of different decomposition products of the inhibitor itself. These differences disappear quickly as the catalytic recombination reaction cycles equilibrate the relative levels of PO_2, HOPO and $HOPO_2$. The relative levels of these OPCs in the products is determined by their equilibrium constants and the overall equivalence ratio in the flame, not by the structure or composition of the OPC additive.

These computations demonstrate that flame inhibition kinetics for both additives depend on the reactions and thermochemistry of HOPO, $HOPO_2$, PO_2 and other small species, not on details of the molecular structure of the initial organophosphorus compound. The inhibition

mechanism for compounds in Fig. 5 is the same set of catalytic recombination reactions, and the only distinction between different organophosphate inhibitors appears to be how rapidly these catalytic cycles are established in a given flame. The different inhibitors in Fig. 5 have different hydrocarbon contents, and this will have a minor influence on their inhibition efficiencies because their different C/H/O compositions can affect the equilibrium between HOPO and $HOPO_2$, and additional components such as F atoms will also have minor influences on inhibition efficiencies. However, as shown in Fig. 5-7, the primary inhibition mechanisms for all of these organophosphorus compounds are exactly the same. Flames with TMP additive initially generate $HOPO_2$, while DMMP initially produces HOPO, yet both inhibit the propane flames nearly identically because of the rapid interconversion of the small P-containing species.

Coupling between HOPO and $HOPO_2$ is dominated by the same reactions responsible for flame inhibition. The basic inhibitor reactions catalytically convert $HOPO_2$ and HOPO into PO_2 via the consumption of H, OH and O and then back to $HOPO_2$ and HOPO via consumption of OH and H. The net reactions are conversion of radicals H, OH and O into H_2O and H_2, thereby reducing the radical pool available to propagate the flame. The dominant cycles of inhibition can still be represented by reactions 1 and 2 but they should be viewed as global reactions involving multiple pathways, with chemically activated intermediates such as $PO(OH)_2$ and HPO(OH)O that may be collisionally stabilized during individual trips through the cycles. Since both cycles share the same PO_2 intermediate catalytic species, it is not surprising that $HOPO_2$ and HOPO are quickly interconverted as shown in Figs. 6 and 7. The resulting inhibition mechanism can be summarized by generalization of the original Twarowski model:

$H + PO_2 + M \rightarrow HOPO + M$ (1a)

$HOPO + H \rightarrow H_2 + PO_2$ (1b)

$HOPO + OH \rightarrow H_2O + PO_2$ (1c)

$OH + PO_2 + M \rightarrow HOPO_2 + M$ (2a)

$HOPO_2 + H \rightarrow H_2O + PO_2$ (2b)

$HOPO_2 + H \leftrightarrow HPO(OH)O \leftrightarrow PO(OH)_2 \rightarrow H_2O + PO_2$ (2b')

$HOPO_2 + H \leftrightarrow PO(OH)_2 \rightarrow H_2O + PO_2$ (2b")

We have discussed the complexity of reaction 2 where the second half of the inhibition cycle takes place on a complicated potential energy surface. The same situation applies to the other reactions 1a, 1b and 2a of the Twarowski reactions. In fact, in addition to a direct abstraction reaction, reaction 1c can take place on the same potential energy surface as the second half of cycle 2, with the same overall products but with a different input channel. We have given most attention to the catalytic recombination reaction cycles that produce water, but if H is replaced by other hydrocarbon radicals in these recombination cycles, radical recombination can form methane, methanol and other stable species, which will also result in flame inhibition.

Conclusions

A study of flame inhibition in propane flames by organophosphorus compounds has been carried out experimentally and numerically, with particular attention to variations in inhibition between rich and lean conditions. Species profiles for PO_xH_y species, as well as OPC dopant were measured for TMP in rich and lean propane flames. Comparisons of species profiles with numerical models gave excellent agreement for the lean flame. Differences remain for the rich

flame, and further work to resolve these discrepancies has been proposed. Overall, both experiment and modeling showed that TMP decomposed early in the flame, with $HOPO_2$ becoming the dominant inhititor species in the lean flame and HOPO becoming dominant in the rich flame. Flame speeds of propane flames with different OPC additives showed very similar inhibition efficiency, and computational comparisons between TMP and DMMP as inhibitors showed very similar behavior. New thermochemistry for the OPCs was calculated, using the BAC-G2 method, and new reaction sequences were added, improving agreement between experiment and calculation. Although the same key catalytic cycles are observed for flames with lean and rich equivalence ratios, there is a systematic variation in details of catalytic reaction sequences involved. These details are incorporated into a more generalized form of the inhibition reaction system originally postulated by Twarowski.

Acknowledgments

The computational work was supported by the Office of Basic Energy Sciences, Division of Chemical Sciences, and performed under the auspices of the U. S. Department of Energy by the University of California, Lawrence Livermore National Laboratory under Contract No. W-7405-Eng-48. The experimental work was carried out with support from the Civilian Research and Development Foundation under grant RC1-2386-NO-02 and by US Army Research Office under grant DAAD 19-00-1-0136, Modification No. P00001. HC acknowledges support from Enterprise Ireland under their Research Scholarship and International Collaboration Programmes.

References

1. Hastie, J.W., and Bonnell, D.W., *Molecular Chemistry of Inhibited Combustion Systems*, National Bureau of Standards, NBSIR 80-2169 (1980).
2. Twarowski, A.J., *Combust. Flame* 94, 91-107 (1993).
3. Twarowski, A.J., *Combust. Flame* 94, 341-348 (1993).
4. Twarowski, A.J., *Combust. Flame* 102, 41-54 (1995).
5. Korobeinichev, O.P., Ilyin, S.B., Mokrushin, V.V., and Shmakov, A.G., *Combust. Sci. Technol.* 116, 51-61 (1996).
6. Korobeinichev, O.P., Shvartsbert, V.M., Chernov, A.A., and Mokrushin, B.B., *Proc. Combust. Inst.* 26, 1035-1042 (1996).
7. Korobeinichev, O.P., Bolshova, T.A., Shvartsberg, V.M., and Chernov, A.A., *Combust. Flame* 125, 744-751 (2001).
8. Westbrook, C. K., *Proc. Combust. Inst.* 19: 127-141 (1982).
9. Westbrook, C.K., *Combust. Sci. Technol.* 34, 201-225 (1983).
10. Smith, O.I., Wang, S.-N., Tseregounis, S., and Westbrook, C.K., Combust. Sci. Technol. 30, 241-271 (1983).
11. Glarborg, P., Kubel, D., Dam-Johansen, K., Chiang, H.-M., and Bozzelli, J.W., *Int. J. Chem. Kinet.* 28, 773-790 (1996).
12. Glaude, P.A., Melius, C., Pitz, W.J., and Westbrook, C.K., *Proc. Combust. Inst.* 29, 2469-2476 (2002).
13. Werner, J.H., and Cool, T.A., *Combust. Flame* 117, 78-98 (1999).
14. Zegers, E.J.P., and Fisher, E.M., Combust. Flame 116, 69-89 (1996).

15. MacDonald, M.A., Jayaweera, T.M., Fisher, E.M., and Gouldin, F.C., Proc. Combust. Inst. 27, 2749-2756 (1998).

16. MacDonald, , M.A., Fisher, E.M., and Gouldin, F.C., *Combust. Flame* 124, 668-683 (2001).

17. Wainner, R.T., McNesby, K.L., Daniel, A.W., Miziolek, A.W., and Babushok, V.I., *Halon Options Technical Working Conference (HOTWC)*, Albuquerque, NM, 2000, pp. 141-153.

18. Nogueira, M.F.N., and Fisher, E.M., *Combust. Flame* 132, 352-363 (2003).

19. Korobeinichev, O.P., Ilyin, S.B., Shvartsbert, V.M., and Chernov, A.A., Combust. Flame 118, 718-726 (1999).

20. Korobeinichev, O.P., Ilyin, S.B., Bolshova, T.A., Shvartsberg, V.M., and Chernov, A.A., *Combust. Flame* 121, 593-609 (2000).

21. Korobeinichev, O.P., Mamaev, A.L., Sokolov, V.V., Bolshova, T.A., and Schvartsberg, V.M., *Halon Options Technical Working Conference (HOTWC)*, Albuquerque, NM, 2001, pp. 173-186.

22. Korobeinichev, O.P., Bolshova, T.A., Shvartsberg, V.M., and Shmakov, A.G., *Halon Options Technical Working Conference (HOTWC)*, Albuquerque, NM, 2002, http://www.bfrl.nist.gov/866/HOTWC/pubs/24_Korobeinichev_et_al.pdf

23. Korobeinichev, O.P., Shvartsberg, V.M., Bolshova, T.A., Ahmakov, A.G., and Knyazkov, D.A., Combust. Expl. Shock Waves 38, 127-133 (2002).

24. Glaude, P.A., Curran, H.J., Pitz, W.J., and Westbrook, C.K., *Proc. Combust. Inst.* 28, 1749-1756 (2000).

25. MacDonald, M.A., Jayaweera, T.M., Fisher, E.M., and Gouldin, F.C., Combust. Flame 116, 166-176 (1999).

26. Jayaweera, T.M., Flame Suppression by Aqueous Solutions, Ph.D. thesis, Cornell University, Ithaca, NY, 2002.

27. Korobeinichev, O.P., Tereshenko, A.G., Emelyanov, I.D., Fedorov, S.Y., Kuibida, L.V., and Lotov, V.V., *Combust. Expl. Shock Waves* 21, 524-530 (1985).

28. Mache, H., and Hebra, A., *Sitzungsber. Osterreich. Akad. Wiss., Abt.* IIa, 150 (1941) 157.

29. Linteris, G.T., and Truett, G.T., *Combust. Flame* 105, 15-27 (1996).

30. van Maaren, A., and deGoey, L.P.H., *Combust. Sci. Technol.* 102, 309-314 (1994).

31. Vagelopoulos, C.M., and Egolfopoulos, F.N., *Proc. Combust. Inst.* 25, 1341-1347 (1994).

32. Dyakov, I.V., Konnov, A.A., de Ruyck, J., Bosschaart, K.J., Brock, E.C.M., and de Goey, L.P.H., *Combust. Sci. Technol.* 172, 81-96 (2001).

33. Kee, R.J., Rupley, F.M., Miller, J.A., Sandia National Laboratories SAND89-8009B (1989).

34. Curran, H.J., *Proceedings of the European Combustion Meeting*, 2003.

35. Melius, C., and Allendorf, M.D., *J. Phys. Chem. A* 104, 2168-2177 (2000).

36. Melius, C., in *Chemistry and Physics of Energetic Materials* (S.N. Bulusu, Ed.), Klumer Academic Publishers, Dorderech, The Netherlands, 1990, p. 21.

37. Mackie, J.C., Bacskay, G.B., and Haworth, N.L., *J. Phys. Chem. A* 106, 10825-10830(2002).

38. Bauschlicher, C.W., *J. Phys. Chem. A* 103 (50), 11126-11129 (1999).

39. N.L. Haworth, G.B. Bacskay and J.C. Mackie, *J. Phys. Chem. A* 106, 1533-1541 (2002).

40. Shmakov, A.G., Korobeinichev, O.P., Bolshova, T.A., Shvartsberg, V.M., *Halon Options Technical Working Conference (HOTWC)*, Albuquerque, NM, 2002, http://www.bfrl.nist.gov/866/HOTWC/pubs/25_Shmakov_et_al.pdf

Figure Captions

1. Spatial variations of stable species in lean ($\phi = 0.9$) propane flame. Symbols - experimental data, curves - computed results.

2. Spatial variations of stable species in rich ($\phi = 1.2$) propane flame. Symbols - experimental data, curves - computed results.

3. Spatial variations of temperature and major P-bearing species in lean flame doped with 1200 ppm TMP. Symbols - experimental data, curves - computed results.

4. Spatial variations of temperature and major P-bearing species in rich flame doped with 1200 ppm TMP. Symbols - experimental data, curves - computed results.

5. Experimentally determined, normalized burning velocity of laminar, stoichiometric propane/air flames due to addition of indicated additives.

6. Computed spatial profiles of major P-bearing species in the lean propane flame. Solid curves are from TMP-doped flame, dashed curves for DMMP-doped flame.

7. Computed spatial profiles of major P-bearing species in the rich propane flame. Solid curves are from TMP-doped flame, dashed curves for DMMP-doped flame.

TABLE 1.
Enthalpies of formation (H_f^o [kcal/mol])for phosphorus species, determined by various methods.

Species	BAC-MP4 [24]	CBS [38]	BAC-G2 (current work)	G3X2 [37]
PO	-3.02	-7.8	-8.83	-9.0
PO_2	-67.6	-70.3	-71.3	-69.6
PO_3	-102.8	-107.5	-107.5	
HOPO	-108.0	-112.4	-111.8	-112.3
$HOPO_2$	-165.0	-171.4	-171.9	-170.5
$PO[OH]_2$	-154.7		-157.9	-158.8
HPO	-18.0	-22.6	-23.0	
HPO_2	-97.1		-101.5	
P_2O_3	-147.2		-157.2	
P_2O_4	-204.3		-217.0	
P_2O_5	-256.2		-271.3	

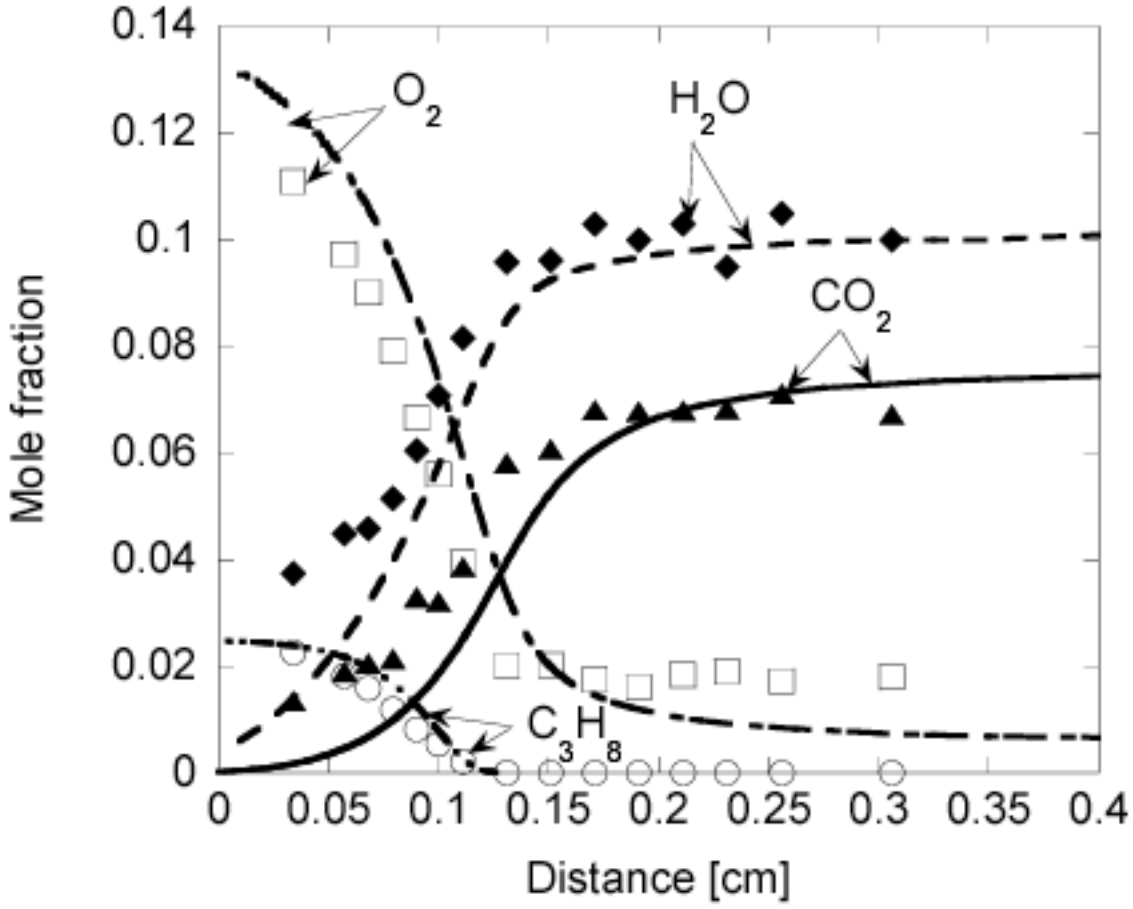
0.14
0.12
0.1
0.08
0.06
0.04
0.02
0
Mole fraction
0
0.05
0.1
0.15
0.2
0.25
0.3
0.35
0.4
Distance [cm]
O2
H2O
CO2
C3H8

Figure 1

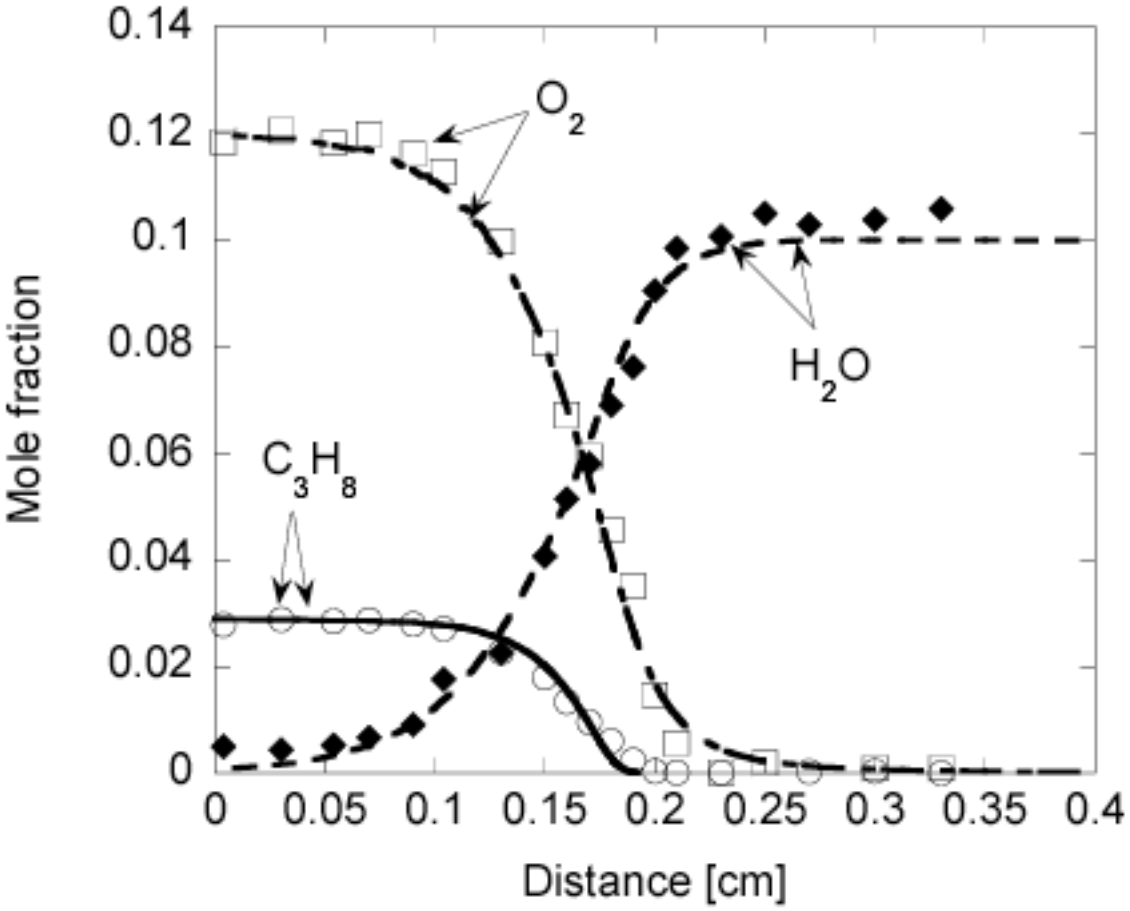
0.14
0.12
0.1
0.08
0.06
0.04
0.02
0
Mole fraction
O2
H2O
C3H8
0
0.05
0.1
0.15
0.2
0.25
0.3
0.35
0.4
Distance [cm]

Figure 2

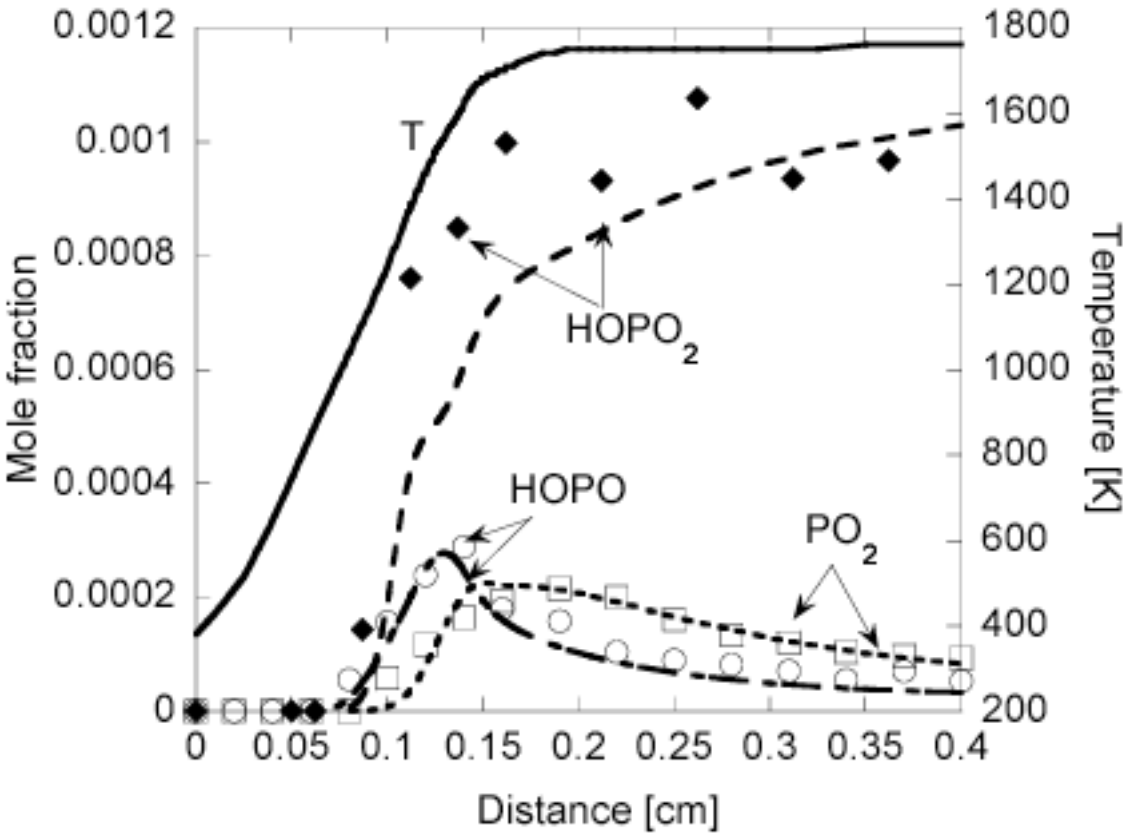
0.0012
0.001
0.0008
0.0006
0.0004
0.0002
0
Mole fraction
1800
1600
1400
1200
1000
800
600
400
200
Temperature [K]
T
HOPO2
HOPO
PO2
0
0.05
0.1
0.15
0.2
0.25
0.3
0.35
0.4
Distance [cm]

Figure 3

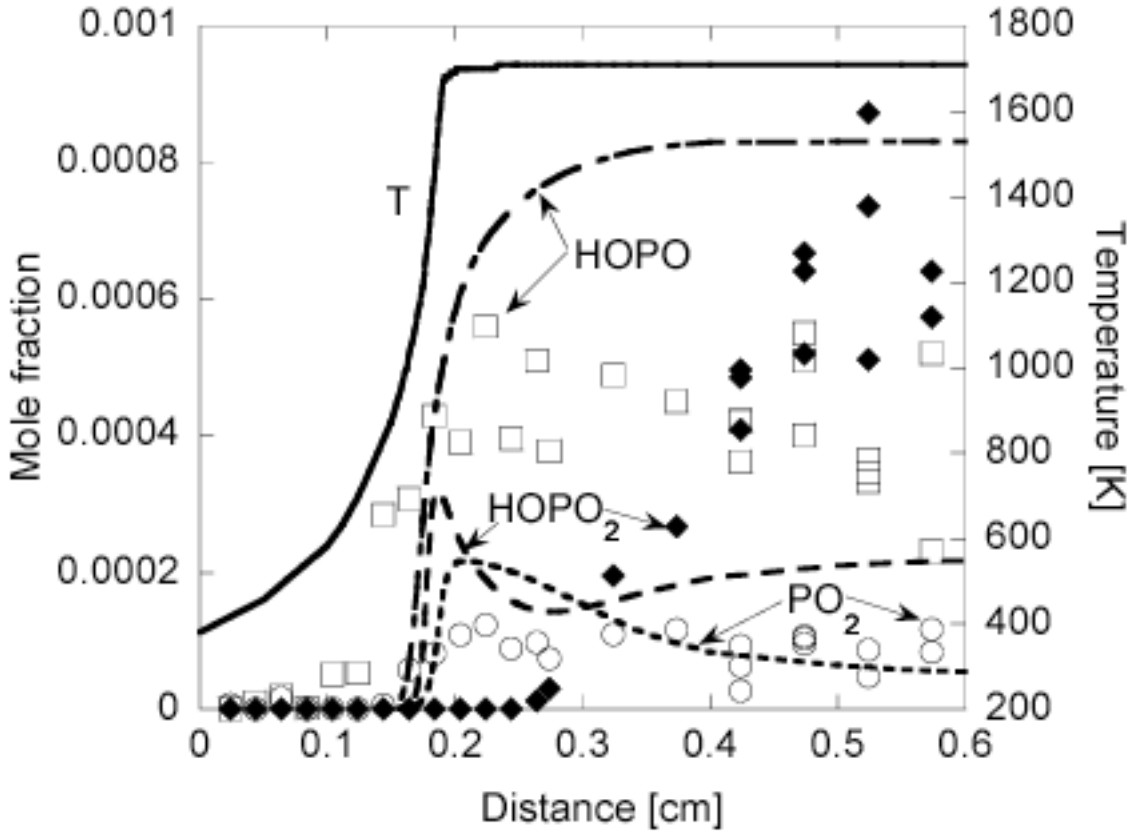
0.001
0.0008
0.0006
0.0004
0.0002
0
Mole fraction
1800
1600
1400
1200
1000
800
600
400
200
Temperature [K]
0
0.1
0.2
0.3
0.4
0.5
0.6
Distance [cm]
T
HOPO
HOPO2
PO2

Figure 4

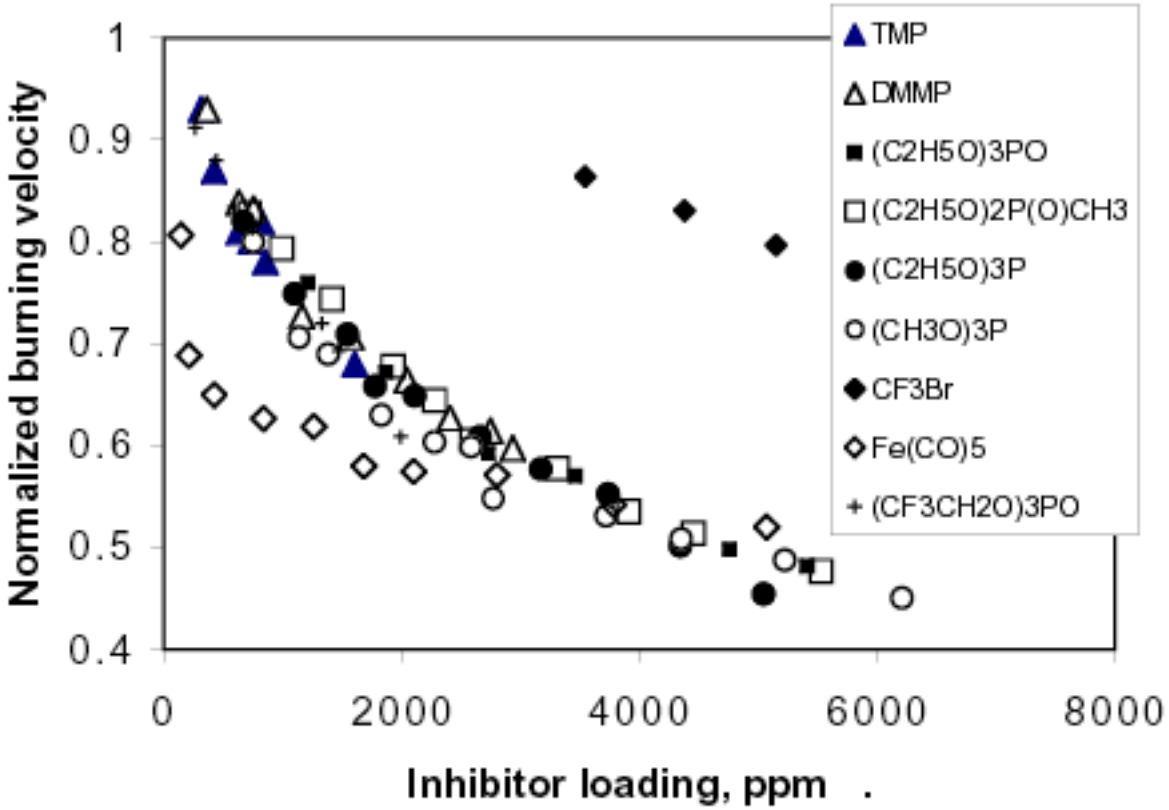
Normalized burning velocity
1
0.9
0.8
0.7
0.6
0.5
0.4
0
2000
4000
6000
8000
Inhibitor loading, ppm
TMP
DMMP
(C2H5O)3PO
(C2H5O)2P(O)CH3
(C2H5O)3P
(CH3O)3P
CF3Br
Fe(CO)5
(CF3CH2O)3PO

Figure 5

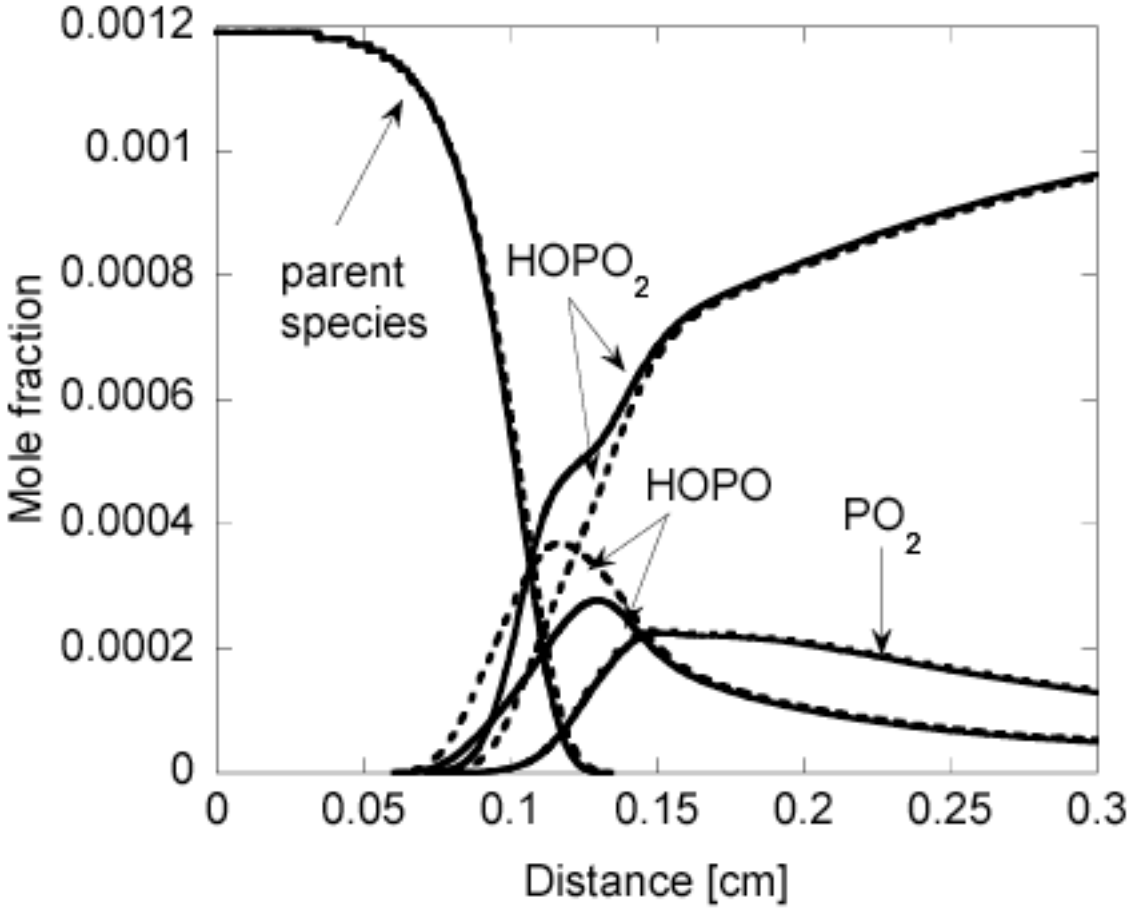
0.0012
0.001
0.0008
0.0006
0.0004
0.0002
0
Mole fraction
parent
species
HOPO2
HOPO
PO2
0
0.05
0.1
0.15
0.2
0.25
0.3
Distance [cm]

Figure 6

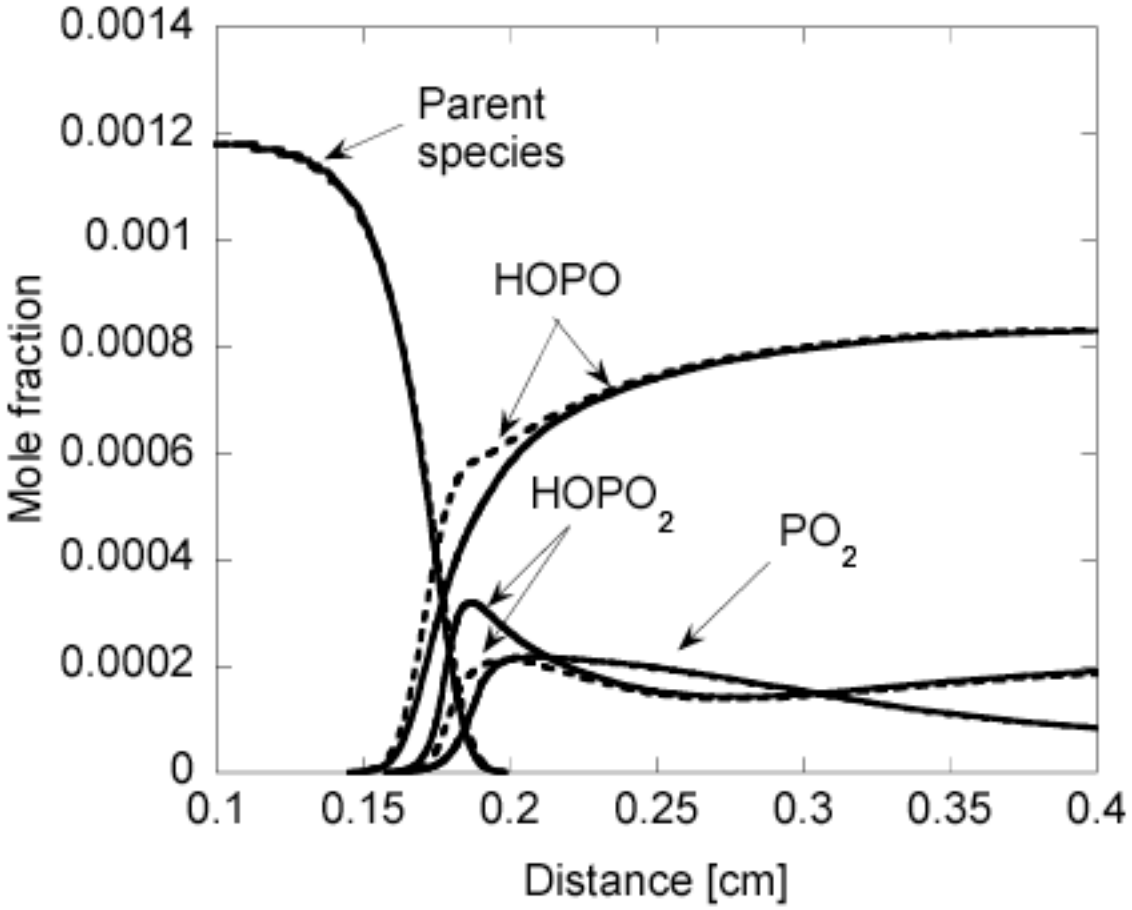
0.0014
0.0012
0.001
0.0008
0.0006
0.0004
0.0002
0
Mole fraction
Parent
species
HOPO
HOPO2
PO2
0.1
0.15
0.2
0.25
0.3
0.35
0.4
Distance [cm]

Figure 7